Uncoupling the MgATP-induced inhibition and aggregation of *Escherichia coli* phosphofructokinase-2 by C-terminal mutations

Mauricio Baez, Felipe Merino, Guadalupe Astorga, Jorge Babul*

Departamento de Biología, Facultad de Ciencias, Universidad de Chile, Santiago, Chile

Abstract **Binding of MgATP to an allosteric site of *Escherichia coli* phosphofructokinase-2 (Pfk-2) provoked inhibition and a dimer–tetramer (D–T) conversion of the enzyme. Successive deletions of up to 10 residues and point mutations at the C-terminal end led to mutants with elevated K_{Mapp} values for MgATP which failed to show the D–T conversion, but were still inhibited by the nucleotide. Y306 was required for the quaternary packing involved in the D–T conversion and the next residue, L307, was crucial for the ternary packing necessary for the catalytic MgATP-binding site. These results show that the D–T conversion could be uncoupled from the conformational changes that lead to the MgATP-induced allosteric inhibition.**

Keywords: Allosteric regulation; Subunit interactions; Substrate inhibition; Pfk-2; Ribokinase superfamily; Dimer–tetramer transition

1. Introduction

Substrate inhibition induced by MgATP is an extended characteristic of phosphofructokinases characterized from different sources. In *Escherichia coli*, two non-homologues phosphofructokinases, Pfk-1 and Pfk-2 [1], have been described to show MgATP-induced substrate inhibition [2–5]. In the case of Pfk-2, this enzymatic inhibition has been related with the presence of an allosteric site for the nucleotide [3], a relevant feature, since *E. coli* strains that express a non-inhibited form of the enzyme presented a diminished growth rate in gluconeogenic media [6].

The quaternary structure of the free form of Pfk-2 has been described as a permanent homodimer whose aggregation state is an obligated conformation necessary for catalysis and stability [7,8]. However, the fact that the presence of MgATP favored the tetrameric form of the enzyme [1,2] prompted the idea that the dimer is the active form of Pfk-2 and the tetramer the inhibited one [9,10]. Nevertheless, the precise role of the tetramer in the inhibition mechanism is still unknown, mainly because of the absence of a model that describes the kinetics of substrate inhibition on the one hand, and the absence of structural support for the biochemical data on the other.

Binding of MgATP to the free enzyme (measured by fluorescence titration) has been interpreted as an allosteric binding [10] because the kinetic mechanism of addition of substrates predicts that MgATP binding to the active site is forbidden in the absence of fructose-6-phosphate (fructose-6-P) [11]. In this regard, a fragment of Pfk-2 obtained by limited proteolysis retained the allosteric-binding capacity, as indicated by fluorescence titration experiments performed in presence of MgATP, but was not able to form tetramers [12]. Since the Pfk-2 fragment was characterized as a ~28 kDa polypeptide with an intact N-terminal sequence, it was suggested that residues from C-terminal region are important for the MgATP-induced tetramerization [12]. However, the relationship between tetramer formation and the MgATP-induced inhibition of the enzyme could not be addressed since the Pfk-2 fragment was inactive.

Pfk-2 belongs to the ribokinase superfamily [13], an extensive family of kinases that phosphorylates a broad range of vitamins and sugars [14]. In this family, the active sites are mostly contained in a structurally conserved $\alpha/\beta/\alpha$-fold and the structural determinants for the nucleoside phosphate donors binding, ATP or ADP, are located at the C-terminal region of this fold [14,15]. Thus, besides the Pfk-2 inactivation provoked by the proteolytic digestion, structural alterations of the catalytic MgATP-binding site can be predicted to occur upon limited proteolysis of the C-terminal end of enzyme.

In this work, we have performed successive C-terminal deletions and point mutations in Pfk-2 in order to characterize the structural determinants of the catalytic ATP-binding site and the structural determinants of the MgATP-induced dimer–tetramer conversion, whose localization at the C-terminal region is predicted by the limited proteolysis experiments mentioned above. The C-terminal mutants were evaluated with respect to their kinetic parameters, sensitivity towards MgATP inhibition and aggregation state. Finally, the results are discussed in the light of the crystal structure of Pfk-2 obtained recently by our group [PDB ID, 3CQD].

2. Materials and methods

2.1. Site-directed mutagenesis; mutants' expression and purification

Site-directed mutagenesis was carried out using the GeneTailor™ Site-Directed Mutagenesis System (Invitrogen) using a pET21d plasmid (Novagen) containing the *pfk-2* gene as template. Oligonucleotides encoding stop codons were used to introduce new translational stop

*Corresponding author. Fax: +56 2 272 6006.
E-mail address: jbabul@uchile.cl (J. Babul).

Abbreviations: Pfk-2, phosphofructokinase-2; R_h, hydrodynamic radius; K_{Mapp}, apparent Michaelis–Menten constant; k_{cat}, catalytic constant; fructose-6-P, fructose-6-phosphate

sites at the appropriate positions in the C-terminal coding region. The mutations were verified by DNA sequencing of both strands. The mutant Pfk-2 enzymes were produced in *E. coli* Bl21 (DE3). Wild-type and mutant enzymes were purified as described by Parducci et al. [16]. However, the D299 mutant could not be purified because of its poor binding to the Cibacron Blue-Sepharose column. In this case, the overexpressed mutant represents about 80% of the total protein, so its k_{cat} values were corrected accordingly.

2.2. Size exclusion chromatography

Experiments were performed with a Waters 1525 HPLC binary pump system, with a Bio-Sil SEC-250 (7.8 mm × 30 cm) column (Bio-Rad, Hercules, CA, USA) equilibrated in a buffer containing 25 mM Tris–HCl, pH 7.6, 200 mM KCl and 1 mM dithiotreitol at the indicated Mg^{2+}, ATP and fructose-6-P concentrations. Protein elution was recorded with the use of an online Waters 2487 UV dual detector. All runs were carried out at a flow rate of 0.8 ml/min. The column was calibrated with the following molecular-mass markers: Vitamin B-12 (1.35 kDa, 8.5 Å hydrodynamic radius, R_h), horse myoglobin (17 kDa, 19 Å R_h), chicken ovalbumin (44 kDa, 30.5 Å R_h), bovine gamma globulin (158 kDa, 41.8 Å R_h) and bovine thyroglobulin (670 kDa, 85 Å R_h). Protein elution volumes were converted to R_h values using the linear relationship obtained with the molecular-mass markers,

$$R_h = 51.8\sqrt{-\log \mathrm{Kav}} - 9.5$$

$$\mathrm{Kav} = \left(\frac{V_e - V_o}{V_t - V_o}\right)$$

where Kav represents the partition constant calculated from the elution volume (V_e), the void volume (V_o) and the total volume of the column (V_t) [17].

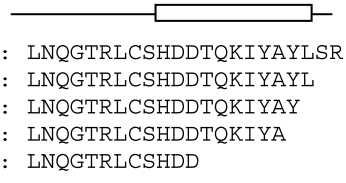

Fig. 1. Successive C-terminal residue deletions of Pfk-2. The C-terminal end α-helix of Pfk-2 is represented with the primary sequence expected for each mutant used in this study.

Table 1
Kinetic parameters measured for the wild-type enzyme and the C-terminal deletion mutants

	Wild-type	L307	Y306	A305	D299
K_{Mapp} fructose-6-P (μM)[a,b]	57 ± 3	60	45	36	20
K_{Mapp} MgATP (μM)[a]	15 ± 3	10	880	800	2000
k_{cat} (s^{-1})[c]	58 ± 3	46	38	35	4

[a]Determinations performed with 1 mM co-substrate.
[b]The concentration of the co-substrate was chosen in order avoid the effect of MgATP binding at the allosteric site to the binding of fructose-6-P to the catalytic site, which is observed above 1 mM MgATP (unpublished observations).
[c]Determinations performed as a function of the MgATP concentration with 1 mM fructose-6-P.

2.3. Enzyme assays

Phosphofructokinase activity was determined spectrophotometrically by coupling the fructose-1,6-bisphosphate production to the oxidation of NADH [1]. The assay was slightly modified to avoid a kinetic lag observed at the initial time of the measurements. Decreasing the Tris–HCl concentration from 100 to 25 mM together the omission of NH_4^+ salt from the assay mixture, eliminates the kinetic lag that complicates the initial velocity measurements at low substrate concentrations, but does not modify the regulatory properties and the k_{cat} values of Pfk-2. The apparent K_M value (K_{Mapp}) for MgATP was calculated by using an uncompetitive substrate inhibition function, and the K_{Mapp} for fructose-6-P by using a non-linear curve fit to a hyperbolic function. The fit procedure was performed by a non-linear regression tool provided by the Sigmaplot package 9.0 (SYSTAT Software Inc).

3. Results

3.1. Dimer–tetramer conversion induced by MgATP and kinetic characterization of the mutants generated by successive removal of residues from the C-terminal end

Four mutants with 2–10 residues deletions from the Pfk-2 C-terminal end (Fig. 1) were characterized with respect to their apparent K_M values for fructose-6-P, MgATP and their catalytic constants (k_{cat}). Compared to the wild-type enzyme, all mutants, with the exception L307, presented increased

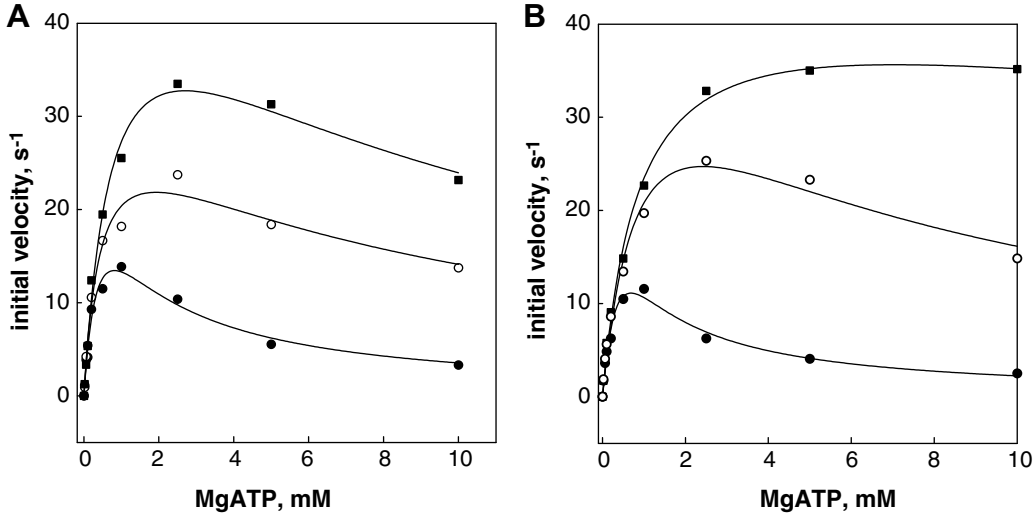

Fig. 2. Activity of the Y306 and A305 mutants as a function of the MgATP concentration. Each panel shows the initial velocity measured as function of the MgATP concentration using a fixed concentration of 2 mM (■), 0.2 mM (○) and 0.05 mM (●) fructose-6-P. Y306 mutant (panel A) and A305 mutant (panel B).

K_{Mapp} values for MgATP without significant changes in the apparent K_M values for fructose-6-P (Table 1). Deletion of three residues (mutant Y306) resulted in a ~1.5 orders of magnitude increase of the K_{Mapp} value for MgATP, with respect to the L307 mutant and the wild-type enzyme. The elimination of L307 seems to be necessary and sufficient to provoke a large alteration in the pseudo-affinity for MgATP, since subsequent deletion of four residues (mutant A305) and 10 residues (mutant D299) lead to a progressive increase, from 1.5 to 1.8 orders of magnitude, of the K_{Mapp} value for MgATP (Table 1). Among the characterized mutants, only Y306 and A305 show a specific alteration in their K_{Mapp} value for MgATP since both mutants retain about the 80% of the wild-type activity without variations of the K_{Mapp} for fructose-6-P (Table 1). Further elimination of up to 10 residues provokes a decrease of the enzymatic activity to 10% of the value of the wild-type enzyme (Table 1).

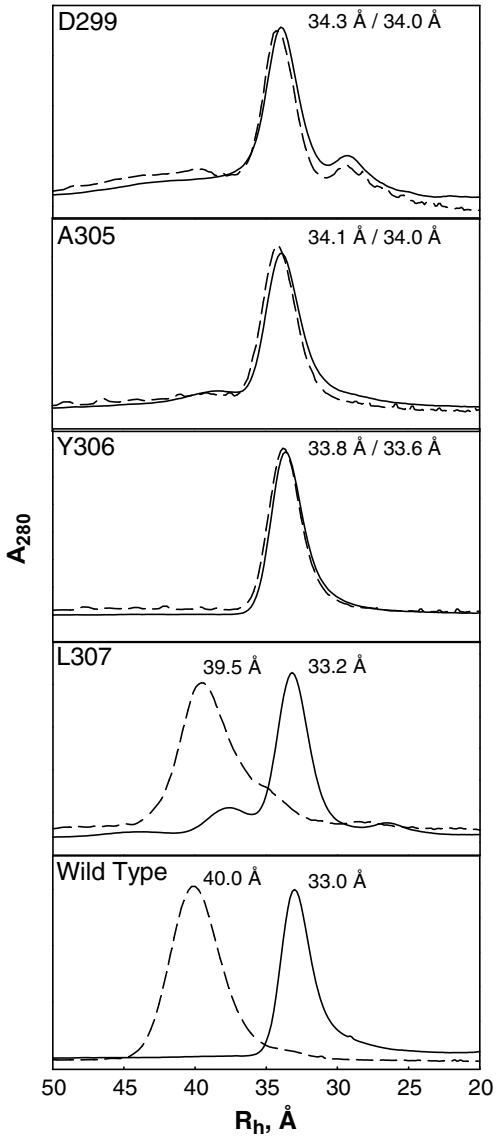

Fig. 3. Effect of MgATP in the agregation state of the wild-type enzyme and the C-terminal mutants. Each panel represents the elution profile of the proteins obtained from a size exclusion chromatography with the column equilibrated without MgATP (segment lines) or with 0.2 mM MgATP (continuous line). The R_h value obtained for each protein is shown into each the panel with (left) or without MgATP (right).

Substrate inhibition induced by MgATP is a property of the wild-type enzyme that has been related with the presence of an allosteric site that negatively regulates the enzymatic activity of Pfk-2 [3,10]. Fig. 2 shows the initial velocity of mutants Y306 and A305 measured as a function of the MgATP concentration by using several fixed concentrations of fructose-6-P. As can be seen, the enzymatic activity goes through a maximum value and then decreases at elevated concentrations of MgATP, indicating that the allosteric inhibition induced by MgATP is still operative, although the K_{Mapp} value for the nucleotide of both mutants was about 1.5 orders of magnitude higher than the wild-type enzyme.

To determine the effect of the C-terminal deletions in the MgATP-induced tetramer formation, size exclusion chromatography was performed in the presence of 0.2 mM MgATP. As shown in Fig. 3, with the exception of the L307 mutant that presents a wild-type phenotype, neither mutant modified significantly its R_h in the presence of 0.2 mM MgATP, suggesting that the structural alterations that resulted in an elevated K_{Mapp} for MgATP are linked with the tetramer formation induced by MgATP binding at the allosteric site. In absence of MgATP the hydrodynamic radiuses of the C-terminal mutants (Y306, A305 and D299) show a slight increment, between 0.6 and 1 Å with respect the value observed for the wild-type dimer (see Fig. 3). Although the observed size increments could be due to alterations in the shape of the mutants or to increments in the tetramer populations, the latter seems unlikely since the dimer–tetramer conversion does not take place in the wild-type enzyme in absence of MgATP [8].

The impediment of those mutants to form tetramers in presence of MgATP, as Y306 and A305, seems not to be related with the enzymatic inhibition induced by MgATP, since both mutants show this feature when the initial velocity is assayed at elevated concentrations of the nucleotide (Fig. 2). In order to study the failure in tetramer formation in a kinetic background closer to the wild-type, the side chains of L307 and Y306 were replaced by alanine to generate the point mutants Y306A and L307A.

3.2. Dimer–tetramer conversion induced by MgATP and kinetic properties of the Y306A and L307A mutants

The MgATP-induced inhibition of Pfk-2 has been described as a biphasic behavior of the initial velocity, measured as function of the MgATP concentration, when the assay was performed at low fructose-6-P concentrations (0.1 mM); which tended to become hyperbolic at elevated concentrations (1 mM) [2,3]. Fig. 4 shows the initial velocity as a function of the MgATP concentration for the wild-type enzyme and the Y306A and L307A mutants using two fixed concentrations of fructose-6-P. At 1 mM fructose-6-P (Fig. 4A), the K_{Mapp} for MgATP for the L307A mutant was about 1.5 orders of magnitude higher than the wild-type enzyme while the k_{cat} and K_{Mapp} for fructose-6-P remain essentially unchanged (Table 2). At 0.1 mM fructose-6-P (Fig. 4B) the MgATP-induced inhibition is favored since a decrease of the initial velocity is observed at elevated concentrations of the nucleotide. As shown, the L307A mutant presents its activity maximum at higher MgATP concentrations compared to the wild-type

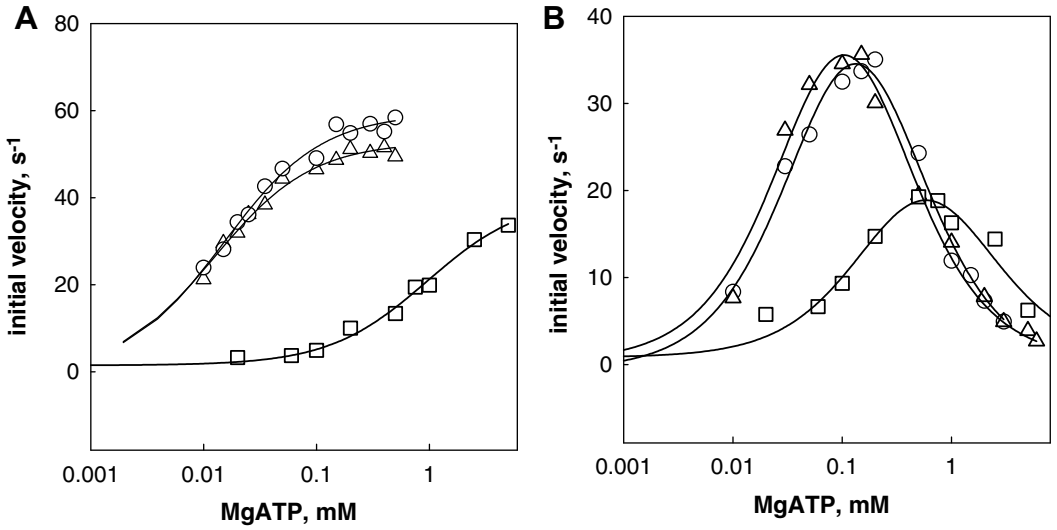

Fig. 4. Dependence of the initial velocity on the MgATP concentrations for wild-type Pfk-2 and the L307A and Y306A mutants. Each panel shows the initial velocity of the L307A mutant (□), Y306A mutant (○) and the wild-type enzyme (△) as function of the MgATP concentration by using fixed concentrations of 2 mM (panel A) and 0.1 mM (panel B) fructose-6-P. The concentration of MgATP is shown in a logarithmic scale.

Table 2
Kinetic parameters measured for the wild-type enzyme and the Y306A and L307A mutants

	Wild-type	Y306A	L307A[b]
K_{Mapp} fructose-6-P (μM)[a]	57 ± 3	62 ± 11	29
K_{Mapp} MgATP (μM)[a]	15 ± 3	13.7 ± 0.9	954
k_{cat} (s^{-1})[c]	58 ± 3	53 ± 3.7	59

[a]Determinations performed with 1 mM co-substrate.
[b]Average of two measurements.
[c]Determinations performed as a function of the MgATP concentration with 1 mM fructose-6-P.

enzyme, probably because of its lower pseudo-affinity for MgATP; the inhibition is still observed although at higher concentrations of the nucleotide. As pointed out above, the C-terminal deletion mutants, characterized by elevated K_{Mapp} values for MgATP, were unable to form tetramers in presence of MgATP. The same situation is observed with the L307A mutant when injected to a size exclusion column in the presence of 0.2 mM MgATP (data not shown). Thus, the origin of the conformational change that leads to an increase in the K_{Mapp} value for MgATP and the impairment in tetramer formation can be mapped to the side chain of L307.

On the other hand, the change of Y306 by alanine does not modify the K_{Mapp} value for MgATP and the other kinetic parameters compared to the wild-type enzyme (Fig. 4A and Table 2). This result seems reasonable since the L307 side chain is present in the protein. However, size exclusion chromatography performed with the Y306A mutant did not show the presence of a tetrameric species even at 0.8 mM MgATP (Fig. 5). Therefore, the side chain of Y306 seems crucial for the MgATP-induced dimer–tetramer conversion, but is not required for the MgATP binding at the active site, as can be deduced from its unaltered K_{Mapp} value. Moreover, since the MgATP-induced inhibition of the enzymatic activity observed in the Y306A mutant was also unmodified with respect to the inhibition pattern of the wild-type (Fig. 4B), the dimer–tetramer conversion seems not to be a requirement for the allosteric inhibition of the Y306A mutant.

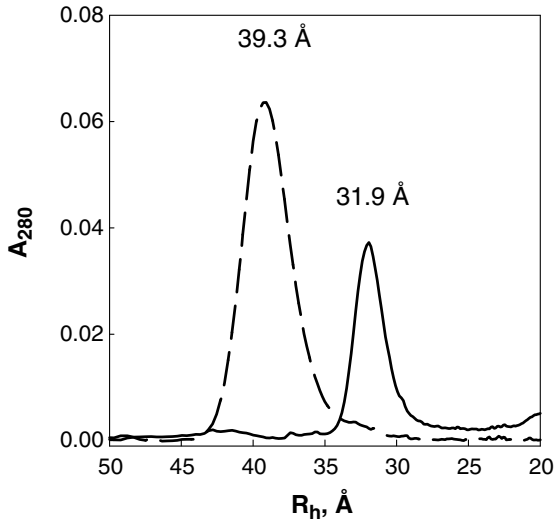

Fig. 5. Effect of MgATP in the hydrodynamic radius (R_h) of the wild-type enzyme and the Y306A mutant. Elution profiles of the wild-type enzyme (dashed line) and the Y306A mutant (continuous line) were obtained by using a size exclusion column equilibrated with 0.8 mM MgATP. The R_h of each species is indicated in the figure.

4. Discussion

4.1. Effect of the successive C-terminal deletions on the kinetic parameters of Pfk-2

Despite of the low sequence identity among the members of the ribokinase superfamily, the nucleotide-binding site is a structurally conserved feature [14,15]. Specifically, the adenine ring of the phosphate donor appears into a hydrophobic pocket created by two loops, the small and large ATP-binding loops, in the ribokinase fold [18]. Fig. 6 shows the C-terminal portion of the crystallographic structure of Pfk-2 where the last segment of eleven residues form an amphipathic α-helix whose hydrophobic side chains are in close contacts with the large ATP-binding loop atoms and with a structurally con-

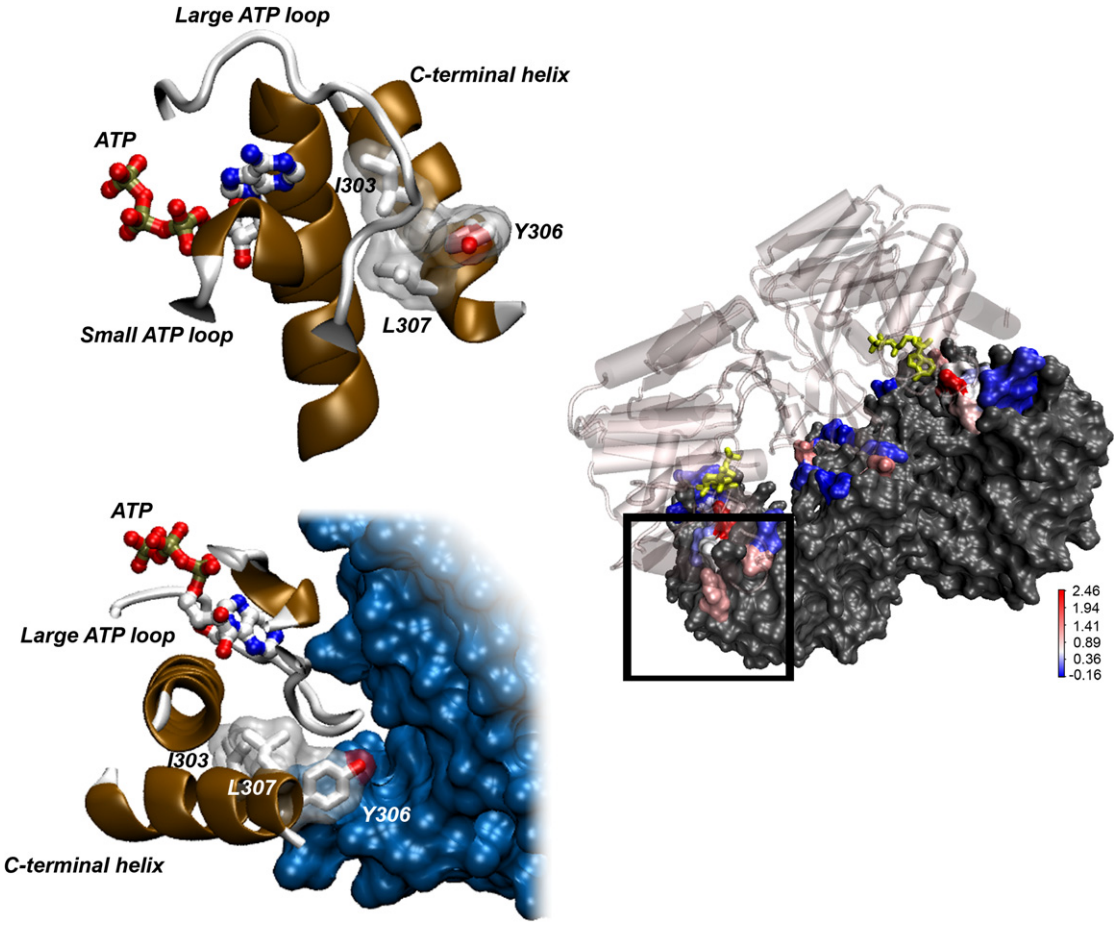

Fig. 6. Relevant structural features of the C-terminal end of Pfk-2. Right: Pfk-2 tetramer [PDB ID, 3CQD]. One homodimer is shown as surface while the other is shown as a cartoon. The portion of the surface drawn dimer in contact with the other dimer is colored based on the $\Delta\Delta G_{bind}$ obtained by the alanine scanning (see Section 4). The catalytic ATP is shown as yellow sticks. The square marks the region highlighted in the left side of the figure. Upper left: tertiary packing of the C-terminal portion of the ATP-binding site. The backbone is shown with ribbon cartoons; the side chains of I303, Y306, and L307 are shown as sticks and surfaces, while the ATP molecule located in the active site is shown as balls and sticks. Bottom left: quaternary packing of the C-terminal region of Pfk-2. The figure shows the contact between Y306 of one dimer with the other dimer. The figure was prepared using the VMD software [24].

served α-helix that participates in the network of the ATP-binding site in the ribokinase superfamily members. Particularly, L307 is the last hydrophobic residue of the amphipathic α-helix whose apolar side chain is buried with atoms of the large ATP loop and of the conserved α-helix (Fig. 6). This feature correlates well with the abrupt increase of 1.5 orders of magnitude of the K_{Mapp} value for MgATP that occurs upon deletion of a three residue segment that includes L307 (mutant Y306) or by a point mutation that replaces its side chain by alanine (mutant L307A). It is known that cavities created by substituting apolar buried side chains by apolar smaller ones, provoke structural rearrangements driven by an unfavorable loss of contacts in hydrophobic cores [19]. The structural rearrangements induced by "cavity-creating" mutants, Y306 and L307A, seems to affect mostly the tertiary packing around the ATP-binding loop since, besides the large increment in the K_{Mapp} value for MgATP, no significant changes were observed in the K_{Mapp} for fructose-6-P or k_{cat} values in these mutants.

Chinese hamster adenosine kinase is a monomeric member of the ribokinase superfamily that shares a 12% sequence identity with Pfk-2, but presents a good alpha carbons structural superposition (1.7 Å R.M.S). Maj and coworkers [20] have performed successive deletions of the C-terminal region of adenosine kinase reporting a gradual decrease of the k_{cat} value together with a progressive increase of the K_{Mapp} for MgATP, while the K_{Mapp} value for the adenosine phosphate acceptor was unaltered, independent of number of deleted residues. Likewise, the K_{Mapp} of the phosphate acceptor of Pfk-2 (fructose-6-P) is maintained with the number of deleted residues, suggesting that conformational changes at the C-terminal region of the ATP-binding site can be uncoupled from the phosphate acceptor-binding site in the ribokinase fold. However, in contrast with the abrupt increase of 1.5 orders of magnitude observed upon deletion of L307 in Pfk-2, in adenosine kinase the K_{Mapp} value for MgATP suffers a gradual increase with the number of deleted residues. The superposition of both structures shows that the deleted residues, in the case of adenosine kinase, form a loop whose side chains do not show direct contacts with atoms involved in the ATP-binding site [21]. Conversely, the hydrophobic side chains of the amphipathic α-helix in Pfk-2 are packed against atoms of the ATP loop and with a helix that forms part of the adenosine-binding moiety (Fig. 6A).

4.2. Effects of the successive C-terminal deletions on the MgATP-induced tetramer formation

A striking characteristic of the C-terminal mutants is that, besides their elevated K_{Mapp} for MgATP, they present impairment in the MgATP-induced tetramer formation. The biologic unit of Pfk-2 present into the crystal structure obtained in the presence of MgATP was assumed to be a homotetramer created by a surface of interaction that hides an extensive area of 2154 $Å^2$ for each dimer (unpublished data). Despite of this extensive contact area, only 4 side chains are expected to decrease the free energy of subunit interaction ($\Delta\Delta G_{bind}$) by at least 1.2 kcal/mol upon alanine replacement. This value was predicted by using an in silico alanine scanning method [22] available in the Web (http://robetta.bakerlab.org/alaninescan). Between the selected side chains, Y306 presents a calculated $\Delta\Delta G_{bind}$ of 4.4 kcal/mol (1.15 kcal/mol per subunit). As shown in Fig. 6, Y306 is the only modified residue in this work whose side chain makes contact with the adjacent homodimer. This suggests that the same conformational change that is responsible for the increased K_{Mapp} value for MgATP, upon replacement or deletion of L307, could modify the correct orientation of the Y306 side chain, which in turn could explain the failure of the dimer–tetramer conversion observed in the "cavity-creating" mutants. In agreement with this idea, the replacement of Y306 by alanine generates a mutant unable to form tetramers, but with a kinetic behavior almost invariant with respect to the wild-type enzyme. The importance of this result is the indication that conformational changes that lead to allosteric inhibition can be uncoupled from tetramer formation at least in the case of the Y306A mutant. For the wild-type enzyme, Cabrera and coworkers [23] reported that, besides tetramer formation, the presence of MgATP promotes subunit conformational changes, defined as rigid movements between the mayor and the minor domains, which result in the closure of the active site of each subunit. Therefore, taking into account that in presence of MgATP the mutant Y306A does not show the dimer–tetramer conversion but presents an inhibition pattern almost undistinguishable from the wild-type enzyme, the enzymatic inhibition induced by MgATP can be explained exclusively by conformational changes at the dimeric or monomeric level of Pfk-2. Further experiments are required to determine the biologic relevance of the dimer–tetramer equilibrium observed in presence of MgATP.

Acknowledgements: This work was supported by a grant from the Comisión Nacional de Investigación Científica y Tecnológica, FONDECYT 1050818, Chile. M.B. is supported by Facultad de Ciencias, Universidad de Chile and FONDECYT. We thank Dr. Victoria Guixé for continuous support and Dr. Ricardo Cabrera for useful discussions.

References

[1] Babul, J. (1978) Phosphofructokinases from *Escherichia coli*. Purification and characterization of the nonallosteric isozyme. J. Biol. Chem. 253, 4350–4355.
[2] Kotlarz, D. and Buc, H. (1981) Regulatory properties of phosphofructokinase 2 from *Escherichia coli*. Eur. J. Biochem. 117, 569–574.
[3] Guixé, V. and Babul, J. (1985) Effect of ATP on phosphofructokinase-2 from *Escherichia coli*. A mutant enzyme altered in the allosteric site for MgATP. J. Biol. Chem. 260, 11001–11005.
[4] Zheng, R.L. and Kemp, R.G. (1992) The mechanism of ATP inhibition of wild type and mutant phosphofructo-1-kinase from *Escherichia coli*. J. Biol. Chem. 267, 23640–23645.
[5] Johnson, J.L. and Reinhart, G.D. (1992) MgATP and fructose 6-phosphate interactions with phosphofructokinase from *Escherichia coli*. Biochemistry 31, 11510–11518.
[6] Torres, J.C., Guixé, V. and Babul, J. (1997) A mutant phosphofructokinase produces a futile cycle during gluconeogenesis in *Escherichia coli*. Biochem. J. 327, 675–684.
[7] Caniuguir, A., Cabrera, R., Baez, M., Vásquez, C., Babul, J. and Guixé, V. (2005) Role of Cys-295 on subunit interactions and allosteric regulation of phosphofructokinase-2 from *Escherichia coli*. FEBS Lett. 579, 2313–2318.
[8] Baez, M., Cabrera, R., Guixé, V. and Babul, J. (2007) Unfolding pathway of the dimeric and tetrameric forms of phosphofructokinase-2 from *Escherichia coli*. Biochemistry 46, 6141–6148.
[9] Guixé, V. and Babul, J. (1988) Influence of ligands on the aggregation of the normal and mutant forms of phosphofructokinase-2 of *Escherichia coli*. Arch. Biochem. Biophys. 264, 519–524.
[10] Guixé, V., Rodriguez, P.H. and Babul, J. (1998) Ligand-induced conformational transitions in *Escherichia coli* phosphofructokinase-2, evidence for an allosteric site for MgATP. Biochemistry 37, 13269–13275.
[11] Campos, G., Guixé, V. and Babul, J. (1984) Kinetic mechanism of phosphofructokinase-2 from *Escherichia coli*. A mutant enzyme with a different mechanism. J. Biol. Chem. 259, 6147–6152.
[12] Cabrera, R., Guixé, V., Alfaro, J., Rodriguez, P.H. and Babul, J. (2002) Ligand-dependent structural changes and limited proteolysis of *Escherichia coli* phosphofructokinase-2. Arch. Biochem. Biophys. 406, 289–295.
[13] Bork, P., Sander, C. and Valencia, A. (1993) Convergent evolution of similar enzymatic function on different protein folds: the hexokinase, ribokinase, and galactokinase families of sugar kinases. Protein Sci. 2, 31–40.
[14] Zhang, Y., Dougherty, M., Downs, D.M. and Ealick, S.E. (2004) Crystal structure of an aminoimidazole riboside kinase from *Salmonella enterica*: implications for the evolution of the ribokinase superfamily. Structure 12, 1809–1821.
[15] Ito, S., Fushinobu, S., Yoshioka, I., Koga, S., Matsuzawa, H. and Wakagi, T. (2001) Structural basis for the ADP-specificity of a novel glucokinase from a hyperthermophilic archeon. Structure 9, 205–214.
[16] Parducci, R.E., Cabrera, R., Baez, M. and Guixé, V. (2006) Evidence for a catalytic $Mg2^+$ ion and effect of phosphate on the activity of *Escherichia coli* phosphofructokinase-2: regulatory properties of a ribokinase family member. Biochemistry 45, 9291–9299.
[17] Laurent, T.C. and Killander, J. (1964) A theory of gel filtration and its experimental verification. J. Chromatogr. 14, 317–330.
[18] Sigrell, J.A., Cameron, A.D., Jones, T.A. and Mowbray, S.L. (1998) Structure of *Escherichia coli* ribokinase in complex with ribose and dinucleotide determined to 1.8 A resolution: insights into a new family of kinase structures. Structure 6, 183–193.
[19] Eriksson, A.E., Baase, W.A., Zhang, X.J., Heinz, D.W., Blaber, M., Baldwin, E.P. and Matthews, B.W. (1992) Response of a protein structure to cavity-creating mutations and its relation to the hydrophobic effect. Science 255, 178–183.
[20] Maj, M.C., Singh, B. and Gupta, R.S. (2000) Structure–activity studies on mammalian adenosine kinase. Biochem. Biophys. Res. Commun. 275, 386–393.
[21] Mathews, I.I., Erion, M.D. and Ealick, S.E. (1998) Structure of human adenosine kinase at 1.5 Å resolution. Biochemistry 37, 15607–15620.
[22] Kortemme, T., Kim, D.E. and Baker, D. (2004) Computational alanine scanning of protein–protein interfaces. Sci. STKE 2004, pl2.
[23] Cabrera, R., Fischer, H., Trapani, S., Craievich, A.F., Garratt, R.C., Guixé, V. and Babul, J. (2003) Domain motions and quaternary packing of phosphofructokinase-2 from *Escherichia coli* studied by small angle X-ray scattering and homology modeling. J. Biol. Chem. 278, 12913–12919.
[24] Humphrey, W., Dalke, A. and Schulten, K. (1996) VMD: visual molecular dynamics. J. Mol. Graph. 14, 33–38.